The Electrophysiological Dynamics of Interference during the Stroop Task

Simon Hanslmayr[1], Bernhard Pastötter[1], Karl-Heinz Bäuml[1], Sieglinde Gruber[2], Maria Wimber[1], and Wolfgang Klimesch[2]

Abstract

■ If subjects are required to name the color of the word *red* printed in blue ink, interference between word meaning and ink color occurs, which slows down reaction time. This effect is well known as the Stroop effect. It is still an unresolved issue how the brain deals with interference in this type of task. To explore this question, an electroencephalogram (EEG) study was carried out. By analyzing several measures of EEG activity, two main findings emerged. First, the event-related potential (ERP) showed increased fronto-central negativity in a time window around 400 msec for incongruent items in contrast to congruent and neutral items. Source localization analysis revealed that a source in the anterior cingulate cortex (ACC) contributed most to the difference. Second, time–frequency analysis showed that theta oscillations (4–7 Hz) in the ACC increased linearly with increasing interference and that phase coupling between the ACC and the left prefrontal cortex was longer persistent for incongruent items compared to congruent and neutral items. These effects occurred at a time window around 600 msec. We conclude that interference between color naming and word meaning in the Stroop task manifests itself at around 400 msec and mainly activates the ACC. Thereafter, sustained phase coupling between the ACC and the prefrontal cortex occurs, which most likely reflects the engagement of cognitive control mechanisms. ■

INTRODUCTION

Imagine you read the word *red* printed in blue ink and your task is to respond to the ink color (blue). Doing so, you'll find yourself engaged in a tricky task. You have to watch yourself carefully not to blurt out the word *red*. Word reading interferes with color naming because reading is a heavily trained ability that occurs almost automatically and, therefore, is hard to suppress. This effect is well known as the Stroop effect (Stroop, 1935), and it is still an open issue how our brain manages interference in this task (for an extensive review, see MacLeod, 1991).

A satisfactory explanation of the Stroop effect would have to answer at least two questions. (i) When does interference occur and (ii) how is interference managed by the brain? Turning to the first question, the main point of interest is whether interference occurs early in time, already at the stimulus processing stage, or late in time closer to the response stage? On a behavioral level, this question can be addressed by varying the stimulus onset asynchrony between the relevant (color) and the irrelevant stimulus dimension (word). These studies suggested that Stroop interference may already occur at the stimulus processing stage (Glaser & Glaser, 1982). On the other hand, several electroencephalogram (EEG) studies have shown that incongruent stimuli (*red* printed in blue ink) have no effect on the amplitude or latency of the P300 component (Rosenfeld & Skogsberg, 2006; Ilan & Polich, 1999; Duncan-Johnson & Kopell, 1981) but induce a stronger negativity around 400 msec than neutral stimuli (Markela-Lerenc et al., 2004; Liotti, Woldorff, Perez, & Mayberg, 2000; Rebai, Bernard, & Lannou, 1997), which suggests that interference occurs at a rather late point in time, closer to the response stage than the stimulus processing stage.

Turning to the second question, how interference is managed by the brain after it is detected, functional magnetic resonance imaging (fMRI) studies revealed that interference in the Stroop task mainly activates frontal brain areas such as the anterior cingulate cortex (ACC) and the dorsolateral prefrontal cortex (DLPFC; van Veen & Carter, 2005; Kerns et al., 2004; Zysset, Müller, Lohmann, & von Cramon, 2001; MacDonald, Cohen, Stenger, & Carter, 2000). A number of recent event-related potential (ERP) studies using a dipole seeding approach confirmed these results (Markela-Lerenc et al., 2004; Liotti et al., 2000) and additionally suggest that different neural mechanisms may underlie conflict detection and conflict resolution (West, 2003). It is widely accepted that the ACC, within its monitoring function, plays a crucial role in detecting interference, whereas the DLPFC is specialized to deal with abstract stimulus and response representations held in working memory

[1]Regensburg University, Germany, [2]Salzburg University, Austria

and can thus exert active cognitive control on planned behavior (Petrides, 2005; Botvinick, Cohen, & Carter, 2004; Kerns et al., 2004; West, Bowry, & McConville, 2004; MacDonald et al., 2000). However, it is still unclear how these brain regions interact with each other to overcome interference.

Interaction between distant brain areas is believed to be established by brain oscillations which promote information exchange (Klimesch, Sauseng, & Hanslmayr, 2007; Fries, 2005; Varela, Lachaux, Rodriguez, & Martinerie, 2001). Several studies have shown that these interactions can be investigated by analyzing phase relationships in a certain frequency range (Lachaux, Rodriguez, Martinerie, & Varela, 1999; Rodriguez et al., 1999). The general assumption is that information transfer between two cortical areas is enhanced when they show a stable difference in phase as measured by the phase-locking value (PLV; see Varela et al., 2001). It has also been shown that this phase locking or phase coupling is positively correlated with a number of cognitive functions, including memory (Tallon-Baudry, Mandon, Freiwald, & Kreiter, 2004; Fell et al., 2001) and attention (Gross et al., 2004; Tallon-Baudry, 2004).

More specifically, oscillations in the theta frequency range (4–7 Hz) have been shown to be closely related to central executive and working memory processes (Sauseng, Klimesch, Schabus, & Doppelmayr, 2005; Sauseng et al., 2004; Tesche & Karhu, 2000; Klimesch, 1996, 1999; Sarnthein, Petsche, Rappelsberger, Shaw, & vonStein, 1998). For example, theta power, as measured by event-related synchronization (ERS; see Pfurtscheller & Aranibar, 1977), over frontal electrode sites, increases with working memory demands (Jensen & Tesche, 2002). Phase coupling in the theta frequency band has also been found to be increased in tasks investigating working memory (Sarnthein et al., 1998) and central executive processes (Sauseng et al., 2005). Studies investigating the neural sources of theta activity found that fronto-medial theta power is generated by prefrontal areas including the ACC (Onton, Delorme, & Makeig, 2005; Ishii et al., 1999; Gevins et al., 1997). A recently conducted study, which recorded fMRI and EEG simultaneously, set out to investigate the neural generators of theta oscillations during an arithmetic task by correlating the blood oxygenation level-dependent (BOLD) response with theta power (Sammer et al., 2007). Their results revealed a widespread cortical network, involving the ACC, to be correlated with theta power. On the basis of these findings, theta oscillations seem to be an ideal candidate to shed light on the interaction between brain areas activated in the Stroop task.

The aim of the present study was to investigate the temporal dynamics of interference elicited in the Stroop task by analyzing several parameters of EEG activity. First, we investigated the time window when interference is detected by means of ERP analysis. We expected to replicate the findings of previous studies, which found the time window around 400 msec to be critical. Second, we investigated the sources that are activated by the Stroop task by using a dipole seeding approach (BESA). Doing so, we used the knowledge of several fMRI studies, which have reliably shown that the Stroop task activates prefrontal regions, such as the ACC and the DLPFC. We expected the ACC to be selectively activated during the time window of interference detection. Third, we analyzed oscillatory activity by means of event-related synchronization and desynchronization (ERS/ERD), which is a measure of power increase (ERS) or decrease (ERD) in a certain frequency band. On the basis of prior work, we hypothesized that theta oscillations show the most pronounced effects of interference in prefrontal brain regions. Fourth, to investigate the interaction between the neural sources, phase-coupling analysis was applied. According to the hypothesis that interference selectively activates the ACC which thereafter engages the prefrontal cortex (PFC), we expected to find an increase in phase coupling between these sources with increasing interference.

METHODS

Subjects

After excluding four subjects due to heavy artifact contamination of the EEG, a sample of 21 subjects (5 men and 16 women) with a mean age of 24.9 years (range = 20 to 33 years), with no reported history of neurological disease, remained for data analysis. All subjects were right handed and gave written informed consent. They were paid €10 to increase motivation.

Stimulus Procedure

The Stroop task consisted of four different conditions: congruent, neutral, incongruent, and negative priming. In the congruent condition, the German color words ''ROT'' (*red*), ''GRÜN'' (*green*), and ''BLAU'' (*blue*) were printed in their respective ink color. For the neutral condition, three neutral German words: ''PECH'' (*misfortune*), ''LECK'' (*leak*), ''SOLL'' (*debit*) were used. These words were chosen because they consist of four letters and share no initial letter with the color words (R, G, or B). The incongruent condition included six different word–color pairings [''ROT'' (*red*) printed in green or blue ink, ''GRÜN'' (*green*) printed in blue or red ink, and ''BLAU'' (*blue*) printed in red or green ink]. The negative priming condition consisted of the same six stimuli as the incongruent condition. The only difference between the negative priming and the incongruent condition was the ordering of the trial sequence. This was done such that the relevant stimulus dimension (color) during a negative priming trial corresponded to the irrelevant stimulus dimension (word) during the preceding incongruent trial. For example, if the word ''BLUE'' printed in red ink occurred in the preceding trial, then the negative

priming condition was the word ''RED'' in blue ink or ''GREEN'' in blue ink (see Figure 1A). Usually, such a trial sequence leads to an increased interference effect as measured by an increase in reaction time [RT] (Neill, 1978; Dalrymple-Alford & Budayer, 1966). Thus, interference should increase linearly from congruent to negative priming items.

The congruent and neutral conditions consisted of 120 trials each, for the incongruent and negative priming conditions, 60 trials were collected. Stimulus duration was 1000 msec with an interstimulus interval of 2000 msec during which a fixation cross appeared on the screen. The four different conditions were presented in blocks of 80 stimuli in pseudorandomized order. Stimuli where shown on a 19-in. computer screen (70 Hz refresh rate) with a visual angle of 7.5° × 2.9°. Subjects were instructed to respond with a button press of their right hand on a conventional computer keyboard to the ink color of the words and to ignore the word meaning.

Materials

The EEG was acquired with a Neuroscan Synamps 32-channel amplifier with a sampling rate of 1000 Hz and frequencies between 0.15 and 70 Hz (Notch-filter was set to 50 Hz). EEG activity was recorded with a reference placed at the nose tip and was later re-referenced to the average of the two earlobes. Twenty-nine Ag–AgCl electrodes (positioned according to the international 10-20 system) were used, and the vertical electrooculogram (EOG) was recorded from an additional channel to control for eye movements and blinks. Impedances were kept below 15 kΩ. Prior to analysis, EOG correction was applied using the algorithm implemented in BESA (Version 5.1.6, Megis Software, Gräfeling Munich). Remaining artifacts were excluded by visual inspection.

Analysis

To avoid influences of outliers on RT data, the median of the RT was computed for each subject. These data were then delivered to a one-way analysis of variance (ANOVA) with the factor condition (congruent, neutral, incongruent, and negative priming). Two-tailed t tests were used for post hoc comparisons. Trials with incorrect responses were discarded from all further analyses. To reveal whether RT increased linearly with increasing interference, polynomial contrasts where computed.

For ERP analysis, the mean amplitude of two time windows, the N400 (400 to 500 msec) and the late negativity (LN; 600–800 msec), was used. These time intervals were chosen because differences between the four conditions began around 400 msec and were persistent until 800 msec. For statistical analysis, two-way ANOVAs were run with the factors location (frontal, central, temporal, parietal, and occipital) and condition (see above) separately for each time window (N400 and LN). The dependent variable for the ANOVA was the mean amplitude of the pooled electrode positions (frontal: Fp1, F7, F3, Fz, Fp2, F8, F4; central: FC5, FC1, C3, Cz, FC2, FC6, C4;

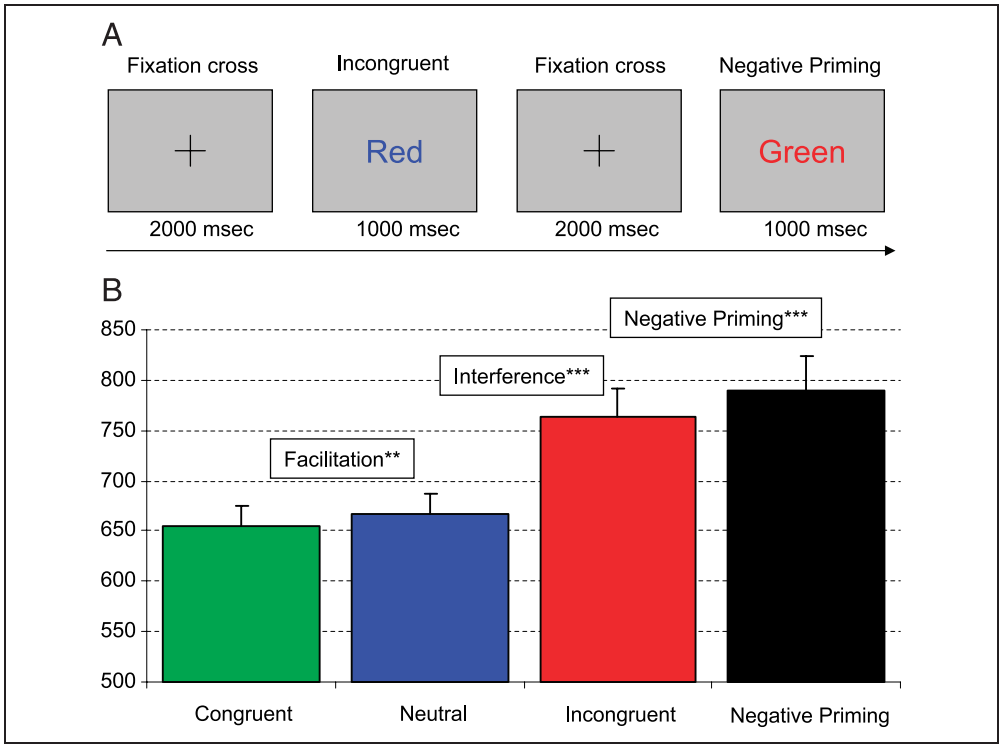

Figure 1. (A) An example of a trial sequence for the negative priming condition is depicted. In the incongruent condition, the word meaning ''red'' has to be ignored, but in the following trial, the subject has to respond to the ink color ''red.'' (B) The mean of the reaction time is plotted for the four different conditions. The results show the classical pattern of facilitation (**$p < .01$), interference (***$p < .001$), and negative priming (**$p < .01$).

temporal: T7, CP5, P7, T8, CP6, P8; parietal: CP1, P3, Pz, P4, CP2; occipital: PO3, PO4, O1, O2). To investigate whether an effect showed a linear increase from congruent to negative priming items, polynomial contrasts were computed. Greenhouse–Geisser correction was applied to all ANOVAs.

BESA Source Localization

BESA uses a dipole seeding approach in which sources are placed into the brain and are then fitted in terms of orientation and/or location in order to explain a maximal amount of variance of the ERP scalp topography. It is important to note that BESA does not produce an inverse solution like other source localization programs, but rather is a tool which works in an interactive fashion and can be used to construct source models, which transform the EEG data from electrode space into source space. The main advantage of this program is that once a source model has been created, the ongoing EEG activity of these sources can be analyzed, which is necessary if induced time–frequency measures (i.e., phase coupling or power) are computed. We created a source model for the grand average of all four conditions. Sources were fitted using a poststimulus interval of 0 to 600 msec, and the criterion for the source model was to explain at least 95% variance of the ERP.

To construct an adequate dipole model, we first placed two bilateral symmetric sources in the left and right occipital cortex (LOC and ROC), which were most reactive to the early evoked visual components (P1/N1). Next, two bilateral symmetric sources were placed in the left and right motor cortex (LMC and RMC) because subjects were required to give manual responses. These sources showed a slow increase in activity in a time window from 400 to 600 msec, which most likely reflects the preparation of a motor response. Thereafter, one source was placed in the ACC. This source was assumed to be active because prior fMRI studies (van Veen & Carter, 2005; Kerns et al., 2004; MacDonald et al., 2000) showed that this brain region is consistently involved in the Stroop task. Following the same rationale, two bilateral symmetric sources were placed in the left and right DLPFC (LPFC and RPFC). An eighth dipole was added to the model, which was placed into the left middle temporal cortex (LMTC). This was done because several studies showed that this area is critically involved in color processing in primates (Buckley, Gaffan, & Mussay, 1997; Horel, 1994) and humans (Miceli et al., 2001; Chao & Martin, 1999). Locations of the eight sources are plotted in Figure 2C, and corresponding Talairach coordinates are shown in Table 1. This model accounted for more than 97% of the variance for all conditions. No additional source could account for another more than 2% variance. Therefore, the model with eight dipoles was used for analysis.

Because it could be argued that nearly every model containing eight sources would explain a considerable amount of variance, we validated the solution with the multiple source probe scan (MSPS) procedure as implemented in BESA 5.1.6. This algorithm is based on the assumption that if the EEG data had been modeled adequately (all active brain regions are represented by the chosen sources), then any additional probe source added to the solution will not show activity apart from noise. The only exception occurs if the probe source is placed close to one of the sources in the current solution. In that case, the probe source and the source in the model share activity of the corresponding brain area. Therefore, if the MSPS algorithm shows only activity around the present sources, it can be inferred that the EEG data have been modeled adequately. This method was also successfully used in a recent combined EEG and fMRI study (Sehatpour, Molohlm, Javitt, & Foxe, 2006).

Statistical Analysis of Source ERPs

Prior to statistical analyses, the orientations of the dipoles were fitted separately for each subject. These data were then delivered to a two-way ANOVA with the factors condition and source, which was calculated separately for each time window. As dependent variable, the mean amplitude of the time window ranging from 400 to 500 msec and 600 to 800 msec was used. This was done because differences between conditions in the grand averages were greatest during this time period, and to make the results comparable to the scalp ERPs.

Event-related Synchronization and Desynchronization

To examine the effect of the Stroop task on brain oscillations, ERS/ERD (Pfurtscheller & Aranibar, 1977) was calculated for the eight sources in a frequency band ranging from 4 to 70 Hz. This measure computes the relative power increase (ERS) or decrease (ERD) of a poststimulus interval relative to a prestimulus baseline. A baseline interval ranging from 750 to 250 msec prior to stimulus onset was used. ERS/ERD was calculated using the algorithm implemented in BESA. To pick up best the activity in each frequency band, the time–frequency resolution was tuned differently for the lower and the higher frequency range. Time–frequency resolution for the lower frequencies (4–20 Hz) was set to 1 Hz and 50 msec, and for the higher frequency ranges (20–70 Hz) to 5 Hz and 10 msec. For statistical comparisons, the data were collapsed for seven frequency bands: Theta (4–7 Hz), lower Alpha (7–10 Hz), upper Alpha (10–13 Hz), Beta 1 (13–20 Hz), Beta 2 (20–30 Hz), Gamma 1 (30–45 Hz), and Gamma 2 (55–70 Hz). These

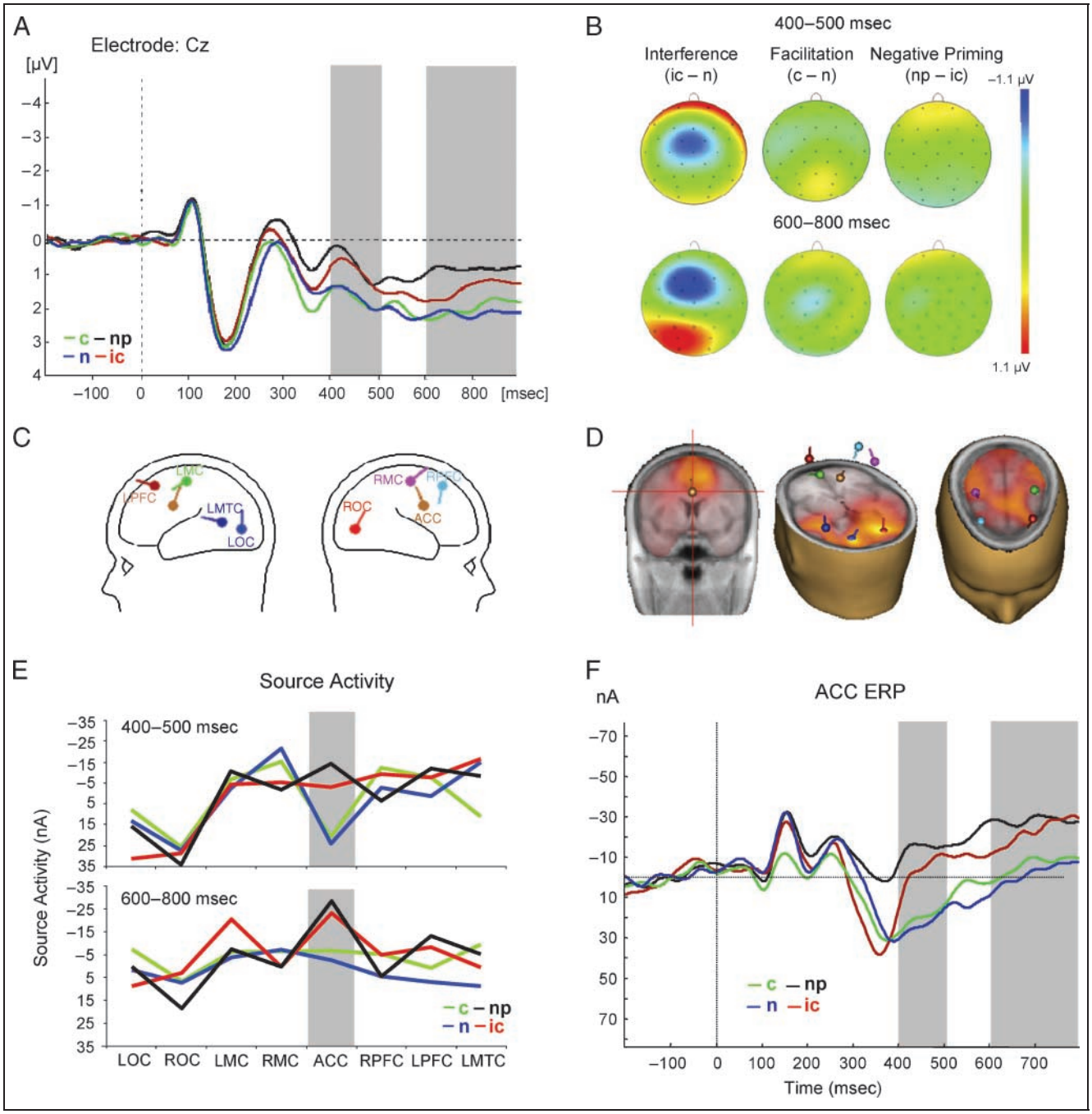

Figure 2. In (A) the ERP of the four different conditions is plotted. The gray bars indicate the time intervals which were used for statistical analysis of the mean amplitude. Scalp maps for the N400 (400–500 msec) and the LN (600–800 msec) time windows are plotted in (B). Compared with neutral items, the incongruent items elicited a more negative potential at fronto-central electrode sites, which was evident for the N400 and the LN time window. Stronger positivity for the incongruent items at fronto-polar sites was observed for the N400 time window, and stronger positivity at left parieto-occipital sites was observed for the LN time window. (C) The sources of the eight localized dipoles are depicted. Two sources were localized in the LOC and ROC, two in the LMC and RMC, one in the ACC, two in the LPFC and RPFC, and one in the LMTC. (D) The results of the MSPS are plotted for the grand average of all conditions. The red color indicates the activity picked up by the MSPS. The activity is located near the eight dipoles, which suggests that the source model is adequate. (E) The mean ERP amplitude for the two time windows (upper panel: N400; lower panel: LN) is plotted for each source. The greatest differences between the conditions appeared in the ACC. (F) The ERP of the ACC source is plotted. The gray bar indicates the time windows used for statistics.

data were collapsed for two consecutive time windows (400–600 msec, 600–800 msec) because interference effects were greatest at this time interval. These data were delivered to three-way ANOVAs with the factors condition, source, and time, which were calculated separately for each frequency band. Only frequency bands which show a main effect for the factor condition will be reported.

Table 1. Talairach Coordinates of the Eight Sources

Brain Region (Abbreviation)	*x*	*y*	*z*
Left occipital cortex (LOC)	−21	−79	−1
Right occipital cortex (ROC)	21	−79	−1
Left motor cortex (LMC)	−36	−17	59
Right motor cortex (RMC)	36	−17	59
Anterior cingulate cortex (ACC)	0	2	33
Left prefrontal cortex (LPFC)	−32	22	57
Right prefrontal cortex (RPFC)	32	22	57
Left middle temporal cortex (LMTC)	−45	−55	9

Phase-coupling Analysis

To examine the effect of the Stroop task on brain connectivity, the PLV was calculated between the localized sources (Varela et al., 2001; Lachaux et al., 1999) using BESA. The PLV estimates the phase coupling of a certain frequency range between two electrode sites or sources. The main advantage of this measure is that it is solely a measure of phase coupling not affected by power changes (e.g., like coherence). The PLV was calculated for the same frequency range as for the ERS/ERD analysis (4–70 Hz). As above, time–frequency resolution for the lower frequencies (4–20 Hz) was set to 1 Hz and 50 msec, and for the higher frequency ranges (20–70 Hz) to 5 Hz and 10 msec. Baseline correction was applied to the PLV values using a time window from 750 to 250 msec prior to stimulus onset.

Because it is known that unequal trial numbers have detrimental effects on time–frequency analysis, especially when measures of phase are involved, the number of trials was held constant between the four conditions for all EEG measures (including ERPs). The procedure for trial selection was such that a random sample of half of the trials was chosen for the neutral and the congruent condition.

Prior to statistical calculation, time–frequency data were collapsed for the time interval ranging from 600 to 800 msec poststimulus because interference effects were most pronounced at this time. To evaluate whether phase coupling differs significantly between conditions, a two-stage procedure was used. At first, one-way ANOVAs with the factor condition were calculated. Thereafter, polynomial contrasts were computed to reveal whether phase locking showed a linear increase or decrease across all four conditions. A given source-pair will only be reported if it revealed significance in both analysis steps ($p < .05$). To minimize the number of statistical comparisons, and because analysis showed that the ACC was the most active source, (see Figures 2E and 3B), we restricted PLV analysis only to source couplings involving the ACC.

RESULTS

Behavioral Data

Results of the RTs are plotted in Figure 1B. The one-way ANOVA revealed a significant effect of condition on RT [$F(3, 60) = 49.9, p < .001$]. Polynomial contrast analysis revealed a linear trend, showing that RTs increased linearly from congruent to negative priming items [$F(1, 20) = 59.597, p < .001$]. Post hoc comparisons showed that subjects had faster RTs in the congruent than in the neutral condition [654 vs. 667 msec; $t(20) = 3.1, p < .01$], slower RTs in the incongruent than in the neutral condition [667 vs. 762 msec; $t(20) = 7.3, p < .001$], and were slower in the negative priming than in the incongruent condition [789 vs. 762 msec; $t(20) = 2.9, p < .01$]. The ANOVA for response accuracy showed that the four conditions differed significantly [$F(3, 60) = 12,1, p < .001$], showing that subjects had more false responses in the incongruent and negative priming conditions (6.4% and 4.0%, respectively) compared to the neutral and congruent ones (1.3% and 2.3%, respectively). For all EEG analyses, only trials with correct responses were used.

ERP Data

Grand averages of the ERPs are plotted in Figure 2A. Because we were mainly interested in the effects of the factor condition, only significant main effects or interactions involving this factor will be reported.

The ANOVA for the N400 time window (400–500 msec) revealed a significant Condition × Location interaction [$F(12, 240) = 4.189, p < .005$]. This interaction involved two effects: (i) stronger negativity in fronto-central regions for incongruent and negative priming items compared to neutral and congruent ones, and (ii) stronger positivity for incongruent and negative priming items compared to neutral and congruent in fronto-polar scalp regions (see Figure 2A and B). Polynomial contrast analysis showed a linear trend for both effects, indicating that fronto-central negativity and fronto-polar positivity increased linearly from congruent to negative priming items [$F(1, 20) = 6.266, p < .05$ and $F(1, 20) = 30.492, p < .001$, respectively]. The simultaneous positivity at fronto-polar and negativity at fronto-central electrode sites suggests that one dipole located in the middle frontal cortex could have generated this pattern.

The ANOVA for the LN time window revealed a significant main effect for the factor condition [$F(3, 60) = 5.366, p < .01$] and a significant Condition × Location interaction [$F(12, 240) = 3.791, p < .01$]. Again, two effects were involved in this interaction: (i) stronger negativity for the incongruent and negative priming items compared to the congruent and neutral ones at fronto-central electrode sites, and (ii) stronger positivity for the incongruent and negative priming condition at parieto-occipital recording sites (see Figure 2B, lower panel). Polynomial contrast analysis revealed that both effects,

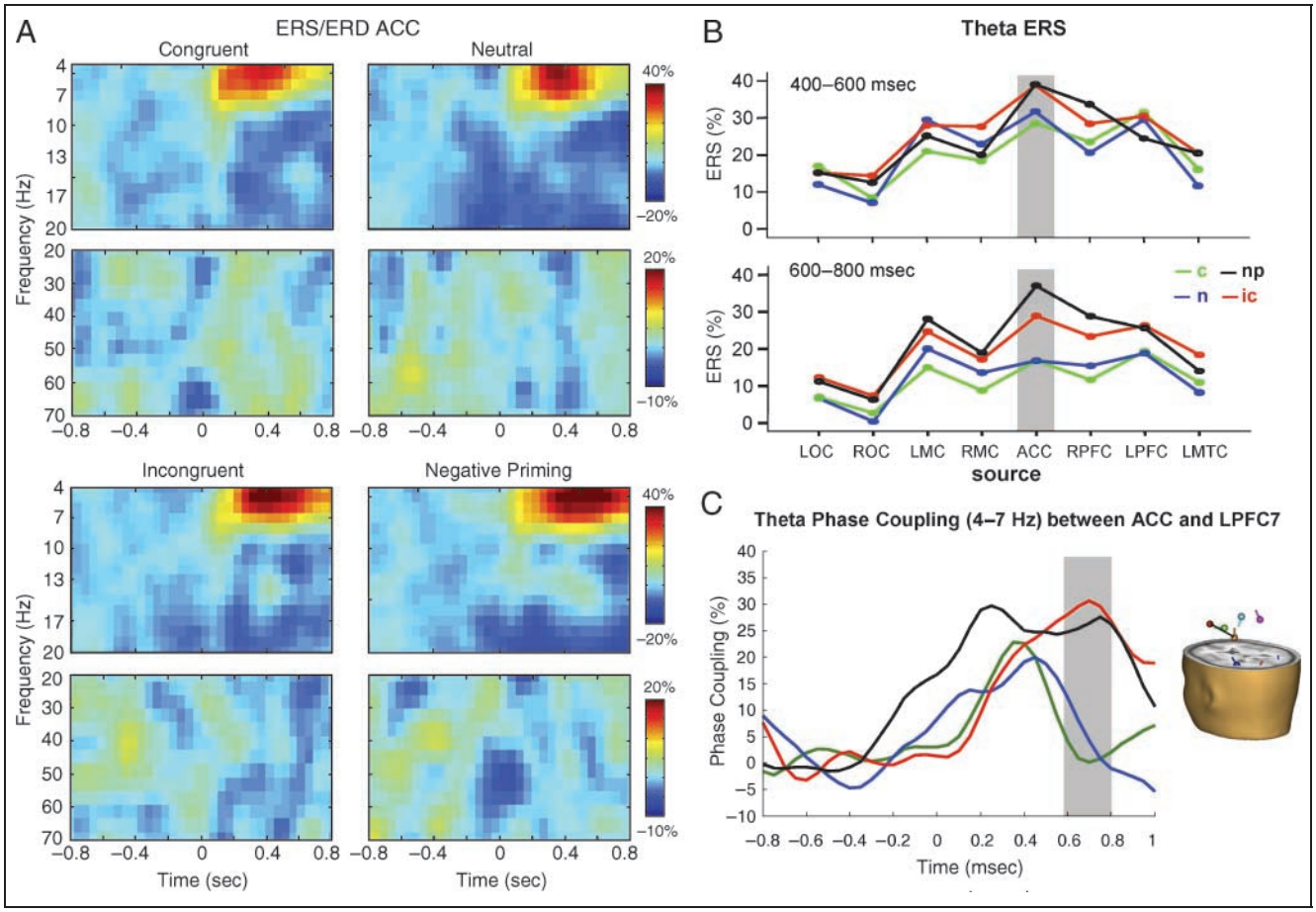

Figure 3. (A) The mean ERS/ERD time–frequency plot for the source of the ACC is shown. Amplitude increase is indicated by hot colors and amplitude decrease is indicated by cold colors. It can be seen that differences between the conditions were most evident in the theta frequency range (4–7 Hz), which shows an increase in ERS from congruent to negative priming items. (B) The mean ERS for all sources is plotted for the early time window (top) and the late time window (bottom). Differences between the four conditions are greatest in the ACC during the late time window (600–800 msec). (C) The time course of the baseline-corrected PLV between the ACC and the LPFC is depicted. Incongruent and negative priming items show stronger phase coupling than congruent and neutral ones in a time window around 600 msec. The gray bar indicates the time window used for statistics. The head model indicates the coupling between the ACC and the LPFC.

fronto-central negativity and parieto-occipital positivity, followed a linear trend [$F(1, 20) = 10.982, p < .005$ and $F(1, 20) = 5.729, p < .05$, respectively].

Source Localization

To investigate the activity of the neural sources of the ERP, BESA dipole localization was carried out (Version 4.2, Megis Software, Gräfeling Munich). The solution of this analysis is plotted in Figure 2C. Talairach coordinates of the sources are shown in Table 1. To investigate the adequateness of this dipole model, an MSPS procedure was applied. Results of the MSPS are plotted in Figure 2D for the grand average of all four conditions. This analysis revealed that the dipole model fitted the data adequately because only activity surrounding the sources of the model was picked up by the MSPS.

By analyzing the ERP source waveforms (from 400 to 500 msec) of the eight localized dipoles, a significant Condition × Source interaction was found [$F(21, 420) = 3.827, p < .001$]. This interaction indicated that the strongest differences between conditions were elicited in the source of the ACC, where negative priming and incongruent trials evoked more negative waveforms than the neutral and congruent ones (see Figure 2E and F). Polynomial contrasts revealed a linear trend for this effect [$F(1, 20) = 14.337, p < .001$], indicating that negativity in the ACC increased linearly with interference. Analysis of the ERP source waveforms for the later time window (600–800 msec) revealed a significant main effect for the factor condition [$F(3, 60) = 3.098, p < .05$] and a marginally significant Condition × Source interaction [$F(21, 420) = 1.983, p = .087$], indicating that the effects for the N400 time window were also persistent for the LN time window (see Figure 2E and F). Again, polynomial contrast analysis revealed that the negativity in the ACC source increased linearly from congruent to negative priming items [$F(1, 20) = 5.951, p < .05$].

Event-related Synchronization and Desynchronization

Theta (4–7 Hz)

The three-way ANOVA for the ERS/ERD data revealed a main effect for condition [$F(3, 60) = 14.576, p < .001$], which was due to stronger ERS for incongruent and negative priming items compared to neutral and congruent ones (see Figure 3A and B). This effect showed a linear trend indicating that ERS increased linearly from congruent to negative priming items [$F(1, 20) = 36.052$, $p < .001$]. Additionally, a significant Condition × Time interaction [$F(3, 60) = 6.221, p < .005$] was obtained, which reflects that differences between the four conditions are more pronounced in the late (600–800 msec) compared to the early time window (Figure 3B). We also found a significant Condition × Time × Source interaction [$F(21, 420) = 1.995, p < .05$], which indicated that the condition effect was strongest in the ACC source during the late time window (see Figure 3B).

Lower Alpha (7–10 Hz)

The ANOVA indicated a significant main effect for the factor condition [$F(3, 60) = 3.134, p < .05$], which also followed a linear trend [$F(1, 20) = 13.554, p < .001$], thus indicating more lower alpha power for the incongruent and negative priming items in contrast to the congruent and neutral ones. No effects for ERD/ERS were observed in the other frequency ranges (see Figure 3A).

Phase Coupling

The ANOVAs for phase-coupling data revealed that a coupling in the theta frequency range (4–7 Hz) between the ACC and the LPFC showed significant differences between the four conditions [$F(3, 60) = 3.707, p < .05$], which followed a linear trend [$F(1, 20) = 7.963, p < .05$]. This effect was due to stronger phase coupling for the incongruent and negative priming conditions compared to the congruent and neutral conditions in a time window ranging from 600 to 800 msec after stimulus presentation (see Figure 3C). Note that theta phase coupling was not correlated with theta ERS/ERD ($r = -.165, p > .45$). Thus, this effect is not artificially created by an increase in theta power. No effects were found in the other frequency ranges or for other source pairings.

DISCUSSION

In this study, we were able to replicate the well-known behavioral pattern of facilitation and interference that has been described in the Stroop literature so many times (MacLeod, 1991). Additionally, we replicated the negative priming effect indicating that interference is even more pronounced in trials in which the irrelevant stimulus dimension of the preceding trial becomes the relevant stimulus dimension. Regarding interference effects in the ERP data, we found that around 400 msec incongruent and negative priming items elicited stronger negativity at fronto-central electrode sites and a stronger positivity at fronto-polar electrodes. The fronto-central negativity was also evident in a later time interval (600–800 msec; Figure 2A and B). This replicates the findings of previous studies (Markela-Lerenc et al., 2004; Liotti et al., 2000; Rebai et al., 1997) and indicates that the time window around 400 msec is sensitive to interference in the Stroop task. Because of its appearance at that time window, this component has also been interpreted to reflect semantic processing, similar to the classical N400 effect (Kutas & Hillyard, 1980).

Dipole source localization revealed that the enhanced fronto-central negativity for incongruent and negative priming items most likely stems from activation of the ACC, which was supported by the selectivity of the source analysis (see Figure 2E). This was most evident for the N400 time interval (400–500 msec), but was also found for the LN time interval (600–800 msec). We conclude that this N400-like effect reflects interference detection and the elicitation of central executive processes rather than the classical semantic incongruency effect. This interpretation has also been suggested by other ERP studies using source localization (e.g., West et al., 2004; West, 2003). Our results are also in line with many fMRI studies showing that the ACC is reliably activated by the Stroop task (for a review, see Botvinick et al., 2004). For instance, MacDonald et al. (2000) showed that the ACC is selectively responding to incongruent stimuli in the Stroop task, whereas the DLPFC is activated during task preparation. Kerns et al. (2004) showed that activity of the ACC during incongruent trials is correlated with the activity of the PFC in the next trial. These studies suggest that the ACC serves monitoring functions and engages the PFC to implement cognitive control. They also suggest an interaction between the ACC and the PFC in order to overcome interference. In sum, the ERP results suggest that the ACC is activated in a time window around 400 msec, which most likely reflects the detection of interference. This activity is elevated until around 800 msec, which might reflect the engagement of central executive processes.

The analysis of the time–frequency data revealed that oscillations in the lower frequency bands (4–10 Hz) were selectively reactive by increasing amplitudes as a function of the degree of interference. This effect was strongest in the theta frequency band (4–7 Hz), but was also found to be present in the neighboring lower alpha band (7–10 Hz). Stronger ERS for incongruent items started to emerge around 400 msec, but was more pronounced in the late time interval (600–800 msec), which is close to the response where maximal interference may occur. The activation of theta oscillations for the incongruent and negative priming condition likely

reflects the activation of central executive processes which are part of our working memory system (Baddeley, 2003). Several other studies showed that theta oscillations are critically related to central executive and working memory processes (Klimesch et al., 2006; Sauseng et al., 2005; Tesche & Karhu, 2000; Sarnthein et al., 1998). Sauseng et al. (2005) observed an increase in fronto-parietal electrode coupling (4–7 Hz) when subjects had to manipulate information stored in working memory. Differences between conditions were strongest in the ACC source, which replicates findings of several other EEG studies showing that theta oscillations, observed over fronto-central electrode sites, have their origin in the ACC (Sauseng, Hoppe, Klimesch, Gerloff, & Hummel, 2007; Onton et al., 2005; Ishii et al., 1999; Gevins et al., 1997).

Concerning the connectivity analysis, we found that phase coupling between the ACC and the LPFC resembled the behavioral pattern of RTs very well. Inspection of the time course of this effect shows that an increase in phase coupling is present for all conditions around 400 msec, but whereas phase coupling drops back to baseline for the congruent and neutral items, it remains elevated for the incongruent and negative priming conditions (see Figure 3C). Phase coupling is believed to be a measure of communication between neural assemblies (Fries, 2005). Physiological investigations of the PFC have demonstrated that Brodmann's areas 9/46 receive their major input from paralimbic regions (anterior and posterior cingulate gyrus) as well as from multimodal temporal association areas, and are thus fitted for the processing of abstract stimulus and response representations (for a review, see Petrides, 2005). Based on this, sustained phase coupling between the ACC and the LPFC may reflect the recruitment and engagement of higher-order control mechanisms which are needed in order to solve interference and to select the proper response. Whereas the response can easily be selected for the congruent and neutral items, a higher level of cognitive control is needed in the incongruent and negative priming conditions. This additional cognitive effort slows down RT. Consistent with this assumption, phase coupling is prolonged for conditions with high interference until the time at which the response to these conditions occurs (around 800 msec). In contrast, phase coupling for conditions with a lower interference level drops back to baseline around the time the response is given (650 msec). Interestingly, phase coupling seems to be slightly more pronounced for the negative priming condition already in the prestimulus interval (see Figure 3C), which might be attributed to the fact that each negative priming condition was preceded by an incongruent item. However, there was no difference between the four conditions in the baseline interval as indicated by a nonsignificant ANOVA [$F(3, 60) < 1$, $p > .5$]. As mentioned above, Kerns et al. (2004) found that BOLD activity in the ACC is correlated with activity in the PFC, which suggests that these two brain regions interact with each other in order to overcome interference. Our results thus are in line with this study and suggest that interference induces sustained coupling between the two cortical regions, which might reflect increased effort to resolve response conflict.

The present study does not claim to localize the exact source of neural activity with high spatial resolution. However, the fact that we found the ACC to be selectively activated during the N400 time window suggests that the activity of the eight different sources could be dissociated well. Also note that dipole seeding approaches can eliminate methodological problems, which cannot be solved on the scalp electrode level. For example, phase coupling between dipole sources is not affected by volume conduction, a confound which cannot be excluded if phase coupling is calculated on an electrode level. More specifically, oscillatory activity in one focal brain region is recorded from several electrodes on the scalp level. If this brain region is more active in one condition and less active in another condition, differences in phase coupling are obtained, which will be misinterpreted to reflect network activity. Hoechstetter et al. (2004) have shown that these problems can be circumvented by applying source modeling. The source localization results, however, should be interpreted with caution, because the exact sources of brain activity cannot be estimated by using EEG.

In sum, our findings give insights into the temporal dynamics of the neural processes activated by interference in the Stroop task. Replicating prior ERP studies, we have shown that interference elicits a negative going ERP around 400 msec. Dipole localization revealed that this effect is most likely generated in the ACC, which is more active for items with a high level of interference (incongruent and negative priming) in contrast to items with a low level of interference (congruent and neutral). Around 200 msec later, the ACC shows an increase in theta power and sustained phase coupling with the LPFC, which presumably reflects the engagement of higher-order control processes in order to resolve response conflict. These results fit well within the framework that considers the ACC to play a crucial role in conflict monitoring and interference detection, resulting in an enhanced prefrontal engagement in conflict control.

Acknowledgments

We thank our colleagues Alp Aslan, Christof Kuhbandner, and Bernhard Spitzer for helpful suggestions. The research was supported by the German Research Foundation (DFG) Grant FOR 448 awarded to Karl-Heinz Bäuml and Wolfgang Klimesch.

Reprint requests should be sent to Simon Hanslmayr, Department of Experimental Psychology, Regensburg University, 93040 Regensburg, Germany, or via e-mail: simon.hanslmayr@psychologie.uni-regensburg.de.

REFERENCES

Baddeley, A. (2003). Working memory: Looking back and looking forward. *Nature Neuroscience Reviews, 4,* 829–839.

Botvinick, M. M., Cohen, J. D., & Carter, C. S. (2004). Conflict monitoring and anterior cingulated cortex: An update. *Trends in Cognitive Sciences, 8,* 439–546.

Buckley, M. J., Gaffan, D., & Mussay, E. A. (1997). Functional double dissociation between two inferior temporal cortical areas: Perirhinal cortex versus middle temporal gyrus. *Journal of Neurophysiology, 77,* 587–598.

Chao, L. L., & Martin, A. (1999). Cortical regions associated with perceiving, naming, and knowing about colors. *Journal of Cognitive Neuroscience, 11,* 25–35.

Dalrymple-Alford, E. C., & Budayer, B. (1966). Examination of some aspects of the Stroop color–word test. *Perceptual and Motor Skills, 23,* 1211–1214.

Duncan-Johnson, C. C., & Kopell, B. S. (1981). The Stroop effect: Brain potentials localize the source of interference. *Science, 214,* 938–940.

Fell, J., Klaver, P., Lehnertz, K., Grunwald, T., Schaller, C., Elger, C. E., et al. (2001). Human memory formation is accompanied by rhinal–hippocampal coupling and decoupling. *Nature Neuroscience, 4,* 1159–1160.

Fries, P. (2005). A mechanism for cognitive dynamics: Neuronal communication through neuronal coherence. *Trends in Cognitive Sciences, 9,* 474–780.

Gevins, A., Smith, M. E., Leong, H., McEvoy, L., Whitfield, S., Du, R., et al. (1997). High-resolution EEG mapping of cortical activation related to working memory: Effects of task difficulty, type of processing, and practice. *Cerebral Cortex, 7,* 374–385.

Glaser, M. O., & Glaser, W. R. (1982). Time course analysis of the Stroop phenomenon. *Journal of Experimental Psychology: Human Perception and Performance, 8,* 875–894.

Gross, J., Schmitz, F., Schnitzler, I., Kessler, K., Shapiro, K., Hommel, B., et al. (2004). Modulation of long-range neural synchrony reflects temporal limitations of visual attention in humans. *Proceedings of the National Academy of Sciences, U.S.A., 101,* 13050–13055.

Hoechstetter, K., Bornfleth, H., Weckesser, D., Ille, N., Berg, P., & Scherg, M. (2004). BESA source coherence: A new method to study cortical oscillatory coupling. *Brain Topography, 16,* 233–238.

Horel, J. A. (1994). Retrieval of color and form during suppression of temporal cortex with cold. *Behavioural Brain Research, 65,* 165–172.

Ilan, A. B., & Polich, J. (1999). P300 and response time from a manual Stroop task. *Clinical Neurophysiology, 110,* 367–373.

Ishii, R., Shinosaki, K., Ukai, S., Inouye, T., Ishihara, T., Yoshimine, T., et al. (1999). Medial prefrontal cortex generates frontal midline theta rhythm. *NeuroReport, 10,* 675–679.

Jensen, O., & Tesche, C. D. (2002). Frontal theta activity in humans increases with memory load in a working memory task. *European Journal of Neuroscience, 15,* 1395–1399.

Kerns, J. G., Cohen, J. D., MacDonald, A. W., III, Cho, R. Y., Stenger, V. A., & Carter, C. S. (2004). Anterior cingulate conflict monitoring and adjustments in control. *Science, 303,* 1023–1026.

Klimesch, W. (1996). Memory processes, brain oscillations and EEG synchronization. *International Journal of Psychophysiology, 24,* 61–100.

Klimesch, W. (1999). EEG alpha and theta oscillations reflect cognitive and memory performance: A review and analysis. *Brain Research Reviews, 29,* 169–195.

Klimesch, W., Hanslmayr, S., Sauseng, P., Gruber, W., Brozinsky, C. J., Kroll, N. E. A., et al. (2006). Oscillatory EEG correlates of episodic trace decay. *Cerebral Cortex, 16,* 280–290.

Klimesch, W., Sauseng, P., & Hanslmayr, S. (2007). EEG alpha oscillations: The inhibition/timing hypothesis. *Brain Research Reviews, 53,* 63–88.

Kutas, M., & Hillyard, S. A. (1980). Reading senseless sentences: Brain potentials reflect semantic incongruity. *Science, 207,* 203–205.

Lachaux, J. P., Rodriguez, E., Martinerie, J., & Varela, F. J. (1999). Measuring phase synchrony in brain signals. *Human Brain Mapping, 8,* 194–208.

Liotti, M., Woldorff, M. G., Perez, R., & Mayberg, H. S. (2000). An ERP study of the temporal course of the Stroop color–word interference effect. *Neuropsychologia, 38,* 701–711.

MacDonald, A. W., III, Cohen, J. D., Stenger, V. A., & Carter, C. S. (2000). Dissociating the role of the dorsolateral prefrontal and the anterior cingulate cortex in cognitive control. *Science, 288,* 1835–1838.

MacLeod, C. M. (1991). Half a century on the Stroop effect: An integrative review. *Psychological Bulletin, 109,* 163–203.

Markela-Lerenc, J., Ille, N., Kaiser, S., Fiedler, P., Mundt, C., & Weisbrod, M. (2004). Prefrontal–cingulate activation during executive control: Which comes first? *Cognitive Brain Research, 18,* 278–287.

Miceli, G., Rouch, E., Capasso, R., Shelton, J. R., Tomaiuolo, F., & Caramazza, A. (2001). The dissociation of color from form and function knowledge. *Nature Neuroscience, 4,* 662–667.

Neill, W. T. (1978). Decision processes in selective attention: Response priming in the Stroop color–word task. *Perception & Psychophysics, 23,* 80–84.

Onton, J., Delorme, A., & Makeig, S. (2005). Frontal midline EEG dynamics during working memory. *Neuroimage, 27,* 341–356.

Petrides, M. (2005). Lateral prefrontal cortex: Architectonic and functional organization. *Philosophical Transactions of the Royal Society of London, 360,* 781–795.

Pfurtscheller, G., & Aranibar, A. (1977). Event-related cortical desynchronization detected by power measurements of scalp EEG. *Electroencephalography and Clinical Neurophysiology, 42,* 817–826.

Rebai, M., Bernard, C., & Lannou, J. (1997). The Stroop's test evokes a negative brain potential, the N400. *International Journal of Neuroscience, 91,* 85–94.

Rodriguez, E., George, N., Lachaux, J. P., Martinerie, J., Renault, B., & Varela, F. J. (1999). Perception's shadow: Long-distance synchronization of human brain activity. *Nature, 397,* 430–433.

Rosenfeld, J. P., & Skogsberg, K. R. (2006). P300-based Stroop study with low probability and target Stroop oddballs: The evidence still favors the response selection hypothesis. *International Journal of Psychophysiology, 60,* 240–250.

Sammer, G., Blecker, C., Gebhardt, H., Bischoff, M., Stark, R., Morgen, K., et al. (2007). Relationship between regional hemodynamic activity and simultaneously recorded EEG-theta associated with mental arithmetic-induced workload. *Human Brain Mapping, 28,* 793–803.

Sarnthein, J., Petsche, H., Rappelsberger, P., Shaw, G. L., & vonStein, A. (1998). Synchronization between prefrontal and posterior association cortex during human working memory. *Proceedings of the National Academy of Sciences, U.S.A., 95,* 7092–7096.

Sauseng, P., Hoppe, J., Klimesch, W., Gerloff, C., & Hummel, F. (2007). Dissociation of sustained attention from central

executive functions: Local activity and interregional connectivity in the theta range. *European Journal of Neuroscience, 25,* 587–593.
Sauseng, P., Klimesch, W., Doppelmayr, M., Hanslmayr, S., Schabus, M., & Gruber, W. R. (2004). Theta coupling in the human electroencephalogram during a working memory task. *Neuroscience Letters, 354,* 123–126.
Sauseng, P., Klimesch, W., Schabus, M., & Doppelmayr, M. (2005). Fronto-parietal EEG coherence in theta and upper alpha reflect central executive functions of working memory. *International Journal of Psychophysiology, 57,* 97–103.
Sehatpour, P., Molohlm, S., Javitt, D. C., & Foxe, J. J. (2006). Spatiotemporal dynamics of human object recognition processing: An integrated high-density electrical mapping and functional imaging study of ''closure'' processes. *Neuroimage, 29,* 605–618.
Stroop, J. R. (1935). Studies of interference in serial verbal reactions. *Journal of Experimental Psychology, 18,* 643–662.
Tallon-Baudry, C. (2004). Attention and awareness in synchrony. *Trends in Cognitive Sciences, 12,* 523–525.
Tallon-Baudry, C., Mandon, S., Freiwald, W. A., & Kreiter, A. K. (2004). Oscillatory synchrony in the monkey temporal lobe correlates with performance in a visual short-term memory task. *Cerebral Cortex, 14,* 713–720.
Tesche, C., & Karhu, J. J. (2000). Theta oscillations index human hippocampal activation during a working memory task. *Proceedings of the National Academy of Sciences, U.S.A., 97,* 919–924.
van Veen, V., & Carter, C. S. (2005). Separating semantic conflict and response conflict in the Stroop task: A functional MRI study. *Neuroimage, 27,* 497–504.
Varela, F., Lachaux, J. P., Rodriguez, E., & Martinerie, J. (2001). The brainweb: Phase synchronization and large-scale integration. *Nature Neuroscience Reviews, 2,* 229–239.
West, R. (2003). Neural correlates of cognitive control and conflict detection in the Stroop and digit-location tasks. *Neuropsychologia, 41,* 1122–1135.
West, R., Bowry, R., & McConville, C. (2004). Sensitivity of medial frontal cortex to response and nonresponse conflict. *Psychophysiology, 41,* 739–748.
Zysset, S., Müller, K., Lohmann, G., & von Cramon, D. Y. (2001). Color–word matching Stroop task: Separating interference and response conflict. *Neuroimage, 13,* 29–36.